CONSTRAINED DESIGN OF ALLPASS TRANSFORMED DFT FILTER-BANKS BY QUADRATIC PROGRAMMING

Heinrich W. Löllmann, Guido Dartmann, and Peter Vary*

Institute of Communication Systems and Data Processing
RWTH Aachen University
52056 Aachen, Germany
{loellmann,vary}@ind.rwth-aachen.de

*Inst. of Communication Technologies and Embedded Systems
RWTH Aachen University
52056 Aachen, Germany
guido.dartmann@ice.rwth-aachen.de

ABSTRACT

A novel numerical design approach for allpass transformed DFT filter-banks with subsampling is proposed. Such frequency warped filter-banks possess a non-uniform time-frequency resolution which is of interest, e.g., for speech and audio processing. The coefficients of the FIR synthesis filters are determined by a constrained least-squares error (CLSE) design. Thereby, the stopband energy of the synthesis filters is minimized with the constraint for perfect reconstruction (PR). This design by quadratic programming accounts also for polyphase network (PPN) filter-banks where the prototype filter degree exceeds the number of subbands to facilitate an enhanced frequency selectivity. In contrast to known designs for allpass transformed analysis-synthesis filter-banks (AS FBs), perfect signal reconstruction can be achieved effectively with synthesis filters featuring a pronounced bandpass characteristic.

Index Terms— allpass transformation, frequency warping, filter-banks, quadratic programming, perfect reconstruction

1. INTRODUCTION

The design of a digital filter-bank with non-uniform time-frequency resolution by means of an allpass transformation is a well-known technique [1]. Such frequency warped filter-banks can mimic the Bark frequency scale, which models the frequency resolution of the human auditory system, with great accuracy [2]. This feature is exploited, among others, for speech enhancement systems, e.g., [3, 4]. One benefit of warped filter-banks is their lower complexity and signal delay in comparison to tree-structured filter-banks whose delay increases exponentially with the number of stages.

The design of allpass transformed *analysis-synthesis filter-banks* (AS FBs) has been addressed by several authors [3–15]. An early approach is to apply the allpass transformation to a uniform FIR analysis-synthesis filter-bank (AS FB), which results IIR analysis *and* synthesis filters. The phase distortions caused by the frequency warping can be (partly) compensated by a phase equalizer at the filter-bank output [3, 10, 12]. Alternatively, the emerging aliasing and linear distortions can be minimized, but not eliminated, by a prototype filter design based on quadratically constrained quadratic programming [5].

Another approach to achieve *near-perfect reconstruction* (NPR) is to use an FIR synthesis filter-bank. The closed-form designs of [9, 10, 13] minimize the linear distortions (but not the aliasing) by phase equalization at the synthesis side. In [4], a least-squares error (LSE) minimization is presented to reduce aliasing and linear distortions caused by the warped analysis filter-bank. A complete aliasing cancellation can be achieved by the constrained least-squares error (CLSE) design of [14], which minimizes linear amplitude and phase distortions with the constraint for a linear time-invariant (LTI) system.

An FIR synthesis filter-bank which achieves *perfect reconstruction* (PR) can be obtained by an analytical closed-form solution, which has been shown independently in [6–8]. A severe drawback of this approach is the missing bandpass characteristic of the synthesis filters (see [8]). This can cause high signal distortions if subband processing takes place. Moreover, these designs cannot be used for a polyphase network (PPN) filter-bank where the degree of the analysis prototype filter exceeds the number of subbands.

In this paper, a novel CLSE design for an allpass transformed PPN DFT AS FB is proposed. It can achieve PR with synthesis filters having a high frequency selectivity. In comparison to a recently proposed unconstrained LSE design for PR [15], the devised synthesis filters have a lower complexity and achieve a higher stopband attenuation due to the constrained optimization.

2. THE ALLPASS TRANSFORMED DFT FILTER-BANK

An allpass transformed digital system is obtained by replacing its delay elements by allpass filters [1]: $z^{-1} \rightarrow A(z)$. For this *allpass transformation*, an allpass filter of first order with system function

$$A(z) = \frac{1 - a^* z}{z - a}, \quad |z| > |a|, \quad a \in \left\{ \mathbb{C} \middle| \, |a| < 1 \right\} \tag{1}$$

and frequency response

$$A\big(e^{j\,\Omega}\big) = \frac{1 - a^* e^{j\,\Omega}}{e^{j\,\Omega} - a} = e^{-j\,\varphi_a(\Omega)} \tag{2}$$

is considered. The asterisk * denotes the conjugate complex value and $\mathbb{C}$ the set of all complex numbers. The M allpass transformed analysis filters of a DFT filter-bank have the transfer functions

$$\widetilde{H}_i(z) = \sum_{n=0}^{L-1} h(n) \cdot W_M^{-n\,i} \cdot A^n(z) \tag{3}$$

with $i \in \{\,0, 1, \ldots, M-1\,\}$ and $W_M = \exp\{-j\,2\,\pi/M\}$ (e.g., [9, 13]). The length of the analysis prototype filter $h(n)$ is assumed to be an integer multiple of M w.l.o.g. so that $L = l_M\,M$. This non-uniform DFT analysis filter-bank can be implemented efficiently by a *polyphase network* (PPN)

$$\widetilde{H}_i(z) = \sum_{\lambda=0}^{M-1} H_\lambda^{(M)}\Big(A^M(z)\Big) \cdot W_M^{-\lambda\,i} \cdot A^\lambda(z) \tag{4}$$

$$H_\lambda^{(M)}\Big(A^M(z)\Big) = \sum_{m=0}^{l_M-1} h(m\,M + \lambda) \cdot A^{m\,M}(z)\,. \tag{5}$$

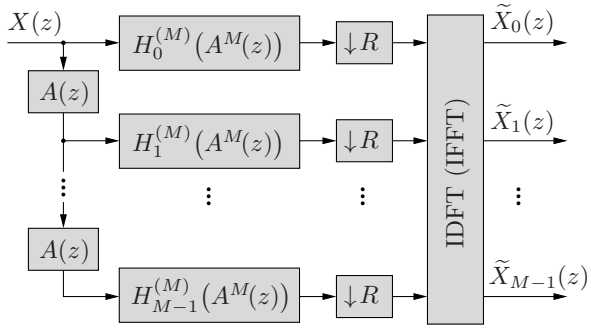

Fig. 1. Polyphase network (PPN) implementation of the allpass transformed DFT analysis filter-bank with downsampling by R.

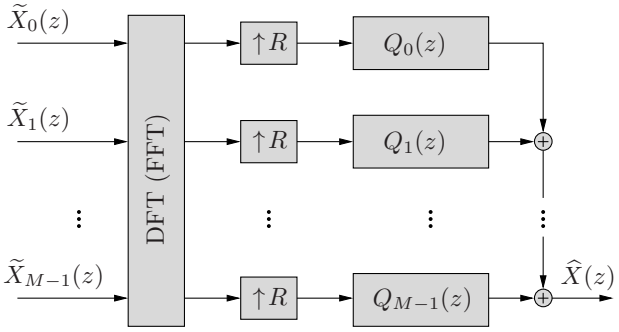

Fig. 2. DFT synthesis filter-bank with upsampling by R.

A diagram of this PPN implementation of the analysis filter-bank is provided by Fig. 1. The inverse discrete Fourier transform (IDFT) can be calculated efficiently by the inverse fast Fourier transform (IFFT). Here, the *same* subsampling rate R is taken for each frequency band so that only the allpass filters must be operated at the input sampling rate where all other operations of the PPN analysis filter-bank are executed at a reduced rate.[1] The *uniform* DFT filter-bank is included as special case for $a = 0$ where $A(z) = z^{-1}$.

The considered FIR synthesis filters are given by

$$F_i(z) = \sum_{\rho=0}^{M-1} W_M^{-i\,(\rho+1)} \cdot Q_{M-1-\rho}(z) \tag{6}$$

$$= \sum_{\rho=0}^{M-1} W_M^{-i\,(\rho+1)} \sum_{n=0}^{N-1} q_{M-1-\rho}(n) \cdot z^{-n} \tag{7}$$

with channel index $i \in \{0, 1, \ldots, M-1\}$. The efficient implementation of this synthesis filter-bank is illustrated in Fig. 2. After some manipulations, Eq. (7) can be expressed by the matrix notation

$$F_i(z) = \boldsymbol{v}_i^T \cdot \boldsymbol{D}^T(z) \cdot \boldsymbol{p} \tag{8a}$$

$$\text{with} \quad \boldsymbol{v}_i = \left[W_M^{-M\,i},\, W_M^{-(M-1)\,i},\, \ldots,\, W_M^{-i} \right]^T \tag{8b}$$

$$\boldsymbol{D}(z) = \boldsymbol{I}_M \otimes \boldsymbol{d}_N(z) \tag{8c}$$

$$\boldsymbol{d}_N(z) = \left[1,\, z^{-1},\, \ldots,\, z^{-(N-1)} \right]^T \tag{8d}$$

$$\boldsymbol{p} = \left[\boldsymbol{q}_0^T,\, \boldsymbol{q}_1^T,\, \ldots,\, \boldsymbol{q}_{M-1}^T \right]^T \tag{8e}$$

$$\boldsymbol{q}_\rho = [\, q_\rho(0),\, q_\rho(1),\, \ldots,\, q_\rho(N-1)\,]^T \tag{8f}$$

$$i, \rho \in \{0, 1, \ldots, M-1\}\,.$$

Bold lower-case variables refer to vectors and matrices are denoted by bold upper-case variables. The superscripts T and H mark the transpose and conjugate transpose of a vector or matrix. The $M \times M$ identity matrix is given by $\boldsymbol{I}_M$ and $\otimes$ marks the Kronecker product of two matrices.

3. NEW SYNTHESIS FILTER-BANK DESIGN

The z-domain representation for the reconstructed input signal of the considered AS FB is given by

$$\widehat{X}(z) = \frac{1}{R} \sum_{r=0}^{R-1} X(z\,W_R^r) \sum_{i=0}^{M-1} \widetilde{H}_i(z\,W_R^r) \cdot F_i(z) \tag{9}$$

[1] This is not fully considered in Fig. 1 for the sake of clarity.

with $R \in \{1, 2, \ldots, M\}$. In general, an AS FB (with subsampling) is a *linear periodically time-varying* (LPTV) system with period R. To account for this behavior, the overall transfer function of the filter-bank is determined by R time-shifted unit sample sequences as input, i.e., $X(z) = z^{-\nu}$ and the reconstructed input signal for this case is denoted by $\widehat{X}_\nu(z)$. Eq. (9) leads now to the new transfer function

$$T_\nu(z) = \frac{\widehat{X}_\nu(z)}{z^{-\nu}} = \frac{1}{R} \sum_{r=0}^{R-1} W_R^{-r\,\nu} \sum_{i=0}^{M-1} \widetilde{H}_i(z\,W_R^r) \cdot F_i(z) \tag{10}$$

with $\nu \in \{0, 1, \ldots, R-1\}$. Inserting Eq. (8a) yields

$$T_\nu(z) = \underbrace{\left(\frac{1}{R} \sum_{r=0}^{R-1} W_R^{-r\,\nu} \sum_{i=0}^{M-1} \widetilde{H}_i\big(z\,W_R^r\big) \cdot \boldsymbol{v}_i^T \cdot \boldsymbol{D}^T(z) \right)}_{\doteq\, \boldsymbol{\xi}_\nu(z) \in \mathbb{C}^{1 \times M\,N}} \cdot \boldsymbol{p}\,. \tag{11}$$

A linear time-invariant (LTI) AS FB with PR is obtained, if the transfer function of Eq. (11) fulfills the conditions

$$T_\nu(z) \stackrel{!}{=} z^{-D_\mathrm{o}} \;\forall\; \nu \in \{0, 1, \ldots, R-1\} \tag{12}$$

where D_o marks the (overall) *signal delay* of the AS FB. The vector notation of Eq. (11) allows to rewrite Eq. (12) as follows

$$\underbrace{\begin{bmatrix} \boldsymbol{\xi}_0(z) \\ \boldsymbol{\xi}_1(z) \\ \vdots \\ \boldsymbol{\xi}_{R-1}(z) \end{bmatrix}}_{\doteq\, \boldsymbol{\Xi}_R(z)} \cdot \boldsymbol{p} \stackrel{!}{=} z^{-D_\mathrm{o}} \cdot \mathbf{1}_R\,. \tag{13}$$

A column vector with R ones is marked by $\mathbf{1}_R$. The requirement of Eq. (13) shall be fulfilled for K discrete z-values on the unit circle

$$z = W_K^\mu = e^{-j\frac{2\pi}{K}\mu}, \quad \mu \in \{0, 1, \ldots, K-1\}\,. \tag{14}$$

With the (stacking) notation

$$\boldsymbol{A} \doteq \begin{bmatrix} \boldsymbol{\Xi}_R(1) \\ \boldsymbol{\Xi}_R(W_K) \\ \vdots \\ \boldsymbol{\Xi}_R\big(W_K^{K-1}\big) \end{bmatrix} \in \mathbb{C}^{K R \times M\,N} \tag{15}$$

$$\boldsymbol{w} \doteq \begin{bmatrix} \mathbf{1}_R \\ W_K^{-D_\mathrm{o}} \cdot \mathbf{1}_R \\ \vdots \\ W_K^{-(K-1)\,D_\mathrm{o}} \cdot \mathbf{1}_R \end{bmatrix} \in \mathbb{C}^{K R \times 1}, \tag{16}$$

Eq. (13) turns now into a set of $K\,R$ linear equations

$$\boldsymbol{A}\boldsymbol{p} = \boldsymbol{w}\,. \tag{17}$$

These equations are overdetermined if $K\,R > M\,N$. In this case, an (unconstrained) *least-squares error* (LSE) solution is given by

$$\widehat{\boldsymbol{p}} = \left(\boldsymbol{A}^H\boldsymbol{A}\right)^{-1}\boldsymbol{A}^H\boldsymbol{w} \tag{18}$$

if the matrix $\boldsymbol{A}^H\boldsymbol{A}$ has full rank. Otherwise a solution exists as well but is non-unique. It should be noticed that the solution of Eq. (18) is not equal to that of [15] where a another synthesis filter-bank with L instead of M sub-filters $Q_\rho(z)$ is considered such that matrices and vector $\boldsymbol{p}$ of Eq. (18) are of lower dimensions than those of [15] for $L > M$. The LSE solution of Eq. (18) strives for a filter-bank with perfect signal reconstruction, but it does not provide necessarily synthesis filters with a sufficient stopband attenuation. Therefore, an additional design constraint is introduced, which minimizes the overall stopband energy of the synthesis filters

$$E_\mathrm{S} = \sum_{i=0}^{M-1} \int\limits_{\Omega\in I_\mathrm{S}(i)} \left|F_i\left(e^{j\,\Omega}\right)\right|^2 \,\mathrm{d}\,\Omega\,. \tag{19}$$

The frequency intervals for the stopbands are given by

$$I_\mathrm{S}(i) = \begin{cases} [\,\Omega_\mathrm{r}(i),\,2\,\pi - \Omega_\mathrm{r}(i)\,] & ,\,i = 0 \\ [\,0,\,\Omega_\mathrm{l}(i)\,] \cup [\,\Omega_\mathrm{r}(i),\,2\,\pi\,] & ,\,i \in \{\,1,\ldots,M-1\,\}. \end{cases} \tag{20}$$

The left and right stopband edges are determined by

$$\Omega_\mathrm{l}(i) = \varphi_a^{[-1]}\left(\frac{2\,\pi}{M}\,i - \frac{\Omega_\mathrm{s}}{2}\right) \tag{21}$$

$$\Omega_\mathrm{r}(i) = \varphi_a^{[-1]}\left(\frac{2\,\pi}{M}\,i + \frac{\Omega_\mathrm{s}}{2}\right) \tag{22}$$

with Ω_s denoting the (normalized) stopband frequency of the original prototype lowpass filter and $\varphi_a^{[-1]}(\Omega)$ marks the inverse function of the allpass phase response of Eq. (2) to account for the warped subband filters. The allpass coefficient of Eq. (2) can be written as

$$a = \alpha e^{j\,\gamma} \quad \text{with} \quad -1 < \alpha < 1, \quad 0 \le \gamma < 2\pi \tag{23}$$

such that the inverse allpass phase response is given by (e.g., [6])

$$\varphi_a^{[-1]}(\Omega) = \gamma + 2\,\arctan\left(\frac{1-\alpha}{1+\alpha}\,\tan\frac{\Omega-\gamma}{2}\right). \tag{24}$$

It is obvious from Eq. (8a) that

$$\left|F_i\left(e^{j\,\Omega}\right)\right|^2 = \boldsymbol{p}^H \cdot \underbrace{\boldsymbol{D}^*\left(e^{j\,\Omega}\right)\cdot\boldsymbol{v}_i^*\cdot\boldsymbol{v}_i^T\cdot\boldsymbol{D}^T\left(e^{j\,\Omega}\right)}_{\doteq\,\boldsymbol{C}_i(\Omega)\,\in\,\mathbb{C}^{M\,N\times M\,N}}\cdot\boldsymbol{p} \tag{25}$$

so that Eq. (19) can be expressed by the matrix formulation

$$E_\mathrm{S} = \boldsymbol{p}^H\cdot\left(\sum_{i=0}^{M-1}\int\limits_{\Omega\in I_\mathrm{S}(i)}\boldsymbol{C}_i(\Omega)\;\mathrm{d}\,\Omega\right)\cdot\boldsymbol{p} = \boldsymbol{p}^H\boldsymbol{S}\boldsymbol{p}\,. \tag{26}$$

The positive definite matrix $\boldsymbol{S} \in \mathbb{R}^{M\,N\times M\,N}$ can be calculated by numerical integration. The vector $\boldsymbol{p}$ with the coefficients of the FIR synthesis filters can now be determined by the following *equality constrained quadratic program* (ECQP)

$$\underset{\boldsymbol{p}}{\text{minimize}}\;\boldsymbol{p}^H\boldsymbol{S}\boldsymbol{p} \quad \text{subject to} \quad \boldsymbol{A}\boldsymbol{p} = \boldsymbol{w}\,. \tag{27}$$

This *convex* optimization problem has a unique optimum and can be solved easily, e.g., by using the function `lsqlin` of the MATLAB optimization toolbox.

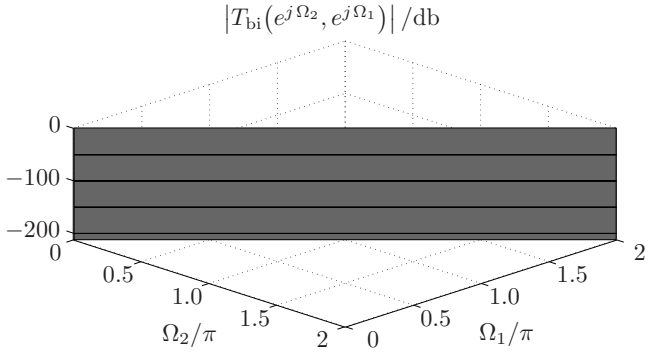

Fig. 3. Magnitude of the bifrequency system function for the new ECQP filter-bank design.

4. DESIGN EXAMPLES

The design of an allpass transformed PPN DFT AS FB with $M = 16$ subbands and analysis prototype lowpass filter

$$h(n) = \frac{\sqrt{R}}{2\,M}\left(1 - \sqrt{2}\,\cos\left(\frac{\pi}{M}(n+0.5)\right)\right) \tag{28a}$$

$$n \in \{0, 1, \ldots, L-1\}, \quad L = 2\,M \tag{28b}$$

is considered, cf., [13].[2] A subsampling rate of $R = 4$ and a real allpass coefficient of $a = 0.4$ are taken. Such an allpass coefficient provides a good approximation of the Bark scale for a sampling frequency of 8 kHz, cf., [2]. The ECQP design of Eq. (27) is performed with parameters $K = M\,N$, $N = 72$, $D_\mathrm{o} = 64$ and $\Omega_\mathrm{s} = 1.1\cdot 2\,\pi/M$.

The obtained solution fulfills the constraints of Eq. (27) with an error norm of $\|\boldsymbol{A}\widehat{\boldsymbol{p}} - \boldsymbol{w}\|_2 = 5.6\cdot 10^{-13}$. This is actually a PR solution given that filter-bank design and implementation have to be performed with finite arithmetic precision in practice. The PR property of the filter-bank becomes obvious by analyzing its transfer functions. A filter-bank is a multi-rate system which can be analyzed by its system response function $t_\mathrm{bi}(k_2, k_1)$, which is the response of a system at time instant k_1 to a unit sample sequence at k_2. The two-dimensional frequency-domain representation is given by the bifrequency system function $T_\mathrm{bi}\left(e^{j\,\Omega_2}, e^{j\,\Omega_1}\right)$ [16], which is plotted in Fig. 3 for the new design. It shows a PR filter-bank since no side-diagonals with alias components occur and the main diagonal, which represents the linear transfer function of the filter-bank, is a straight line. In contrast, the bifrequency system functions of the NPR designs presented in [9, 13] exhibit aliasing as well as linear distortions. The plot of the transfer function of Eq. (10) for $\nu = 0$ in Fig. 4 shows deviations of less than $\pm 1.3\cdot 10^{-13}$ dB. (Such marginal deviations occur also on the main diagonal of Fig. 3.) The phase response of $T_0\left(e^{j\,\Omega}\right)$ is linear and equal to $D_\mathrm{o}\,\Omega$ with deviations of less than $\pm 10^{-13}$ (not plotted). Errors of such magnitude can also be observed for a numerical analysis of the PR filter-banks of [6–8]. In contrast to these closed-form designs, the presented approach also applies for longer analysis prototype filters ($L > M$) and it achieves a distinctive bandpass characteristic for the synthesis filters as demonstrated by Fig. 5.

Fig. 6 exemplifies that the new ECQP design results synthesis filters with a much smaller transition bandwidth than for the unconstrained LSE design of [15] and the closed-form NPR design of [9].

[2] It should be noted that neither the DFT or IDFT of Fig. 1 and Fig. 2 perform a scaling by $1/M$.

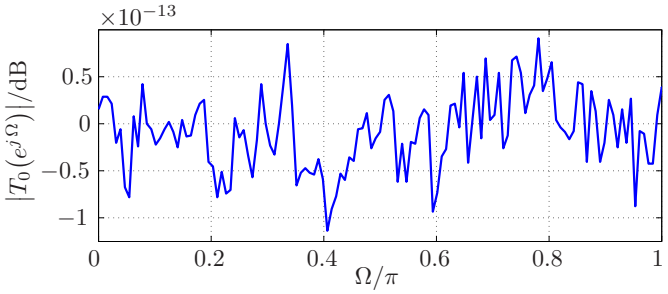

Fig. 4. Magnitude response of transfer function $T_\nu\left(e^{j\,\Omega}\right)$ for $\nu = 0$.

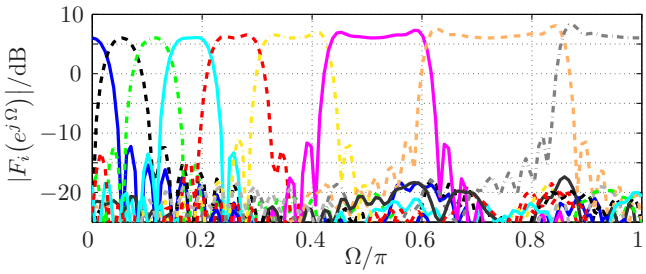

Fig. 5. Magnitude responses of synthesis filters for the new design.

In addition, the design of [9] achieves no PR and exhibits a significantly lower stopband attenuation despite its higher sub-filter degree N and signal delay D_o, respectively: The synthesis lowpass filter of the new design achieves here a stopband energy of only $5.74 \cdot 10^{-3}$ while the stopband energy of the LSE design of [15] equals $9.31 \cdot 10^{-3}$ and that of the NPR design of [9] amounts even to $28.14 \cdot 10^{-3}$. (Similar results are obtained for the other synthesis filters). Thus, the new design can achieve both, PR *and* synthesis filters with a high stopband attenuation. The ability to achieve these targets with high accuracy depends of course on the design parameters where the choice $D_\text{o} = N - 2\,R$ turns out to be favorable.

5. CONCLUSIONS

A novel design of an allpass transformed DFT AS FB with subsampling by means of quadratic programming is presented. The coefficients of the FIR synthesis filters are determined by the design target to minimize their stopband energy with the constraints for PR and a prescribed signal delay. This quadratic LSE minimization with linear equality constraints can be easily solved by common (MATLAB) programs. In contrast to previous NPR designs [3–5, 9–14], the new approach can achieve PR with a high numerical accuracy. Thereby, synthesis filters with a high stopband attenuation are achieved as opposed to the closed-form PR designs of [6–8] and the new design applies also for PPN filter-banks, which enables the use of subband filters with a high frequency selectivity. Due to these properties, the devised non-uniform filter-bank is of special interest for applications such as speech and audio processing.

6. REFERENCES

[1] A. V. Oppenheim, D. Johnson, and K. Steiglitz, "Computation of Spectra with Unequal Resolution Using the Fast Fourier Transform," *Proc. of the IEEE*, vol. 59, no. 2, pp. 299–301, Feb. 1971.

[2] J. O. Smith and J. S. Abel, "Bark and ERB Bilinear Transforms," *IEEE Trans. on Speech and Audio Processing*, vol. 7, no. 6, pp. 697–708, Nov. 1999.

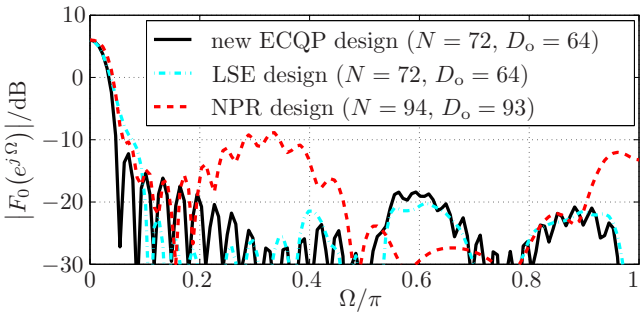

Fig. 6. Magnitude response of synthesis lowpass filter for the new ECQP design, the LSE design of [15] and the NPR design of [9].

[3] T. Gülzow, A. Engelsberg, and U. Heute, "Comparison of a Discrete Wavelet Transformation and a Nonuniform Polyphase Filterbank applied to Spectral-Subtraction Speech Enhancement," *Signal Processing*, vol. 64, no. 1, pp. 5–19, Jan. 1998.

[4] J. M. de Haan, I. Claesson, and H. Gustafsson, "Least Squares Design of Nonuniform Filter Banks with Evaluation in Speech Enhancement," in *Proc. of Intl. Conference on Acoustics, Speech, and Signal Processing (ICASSP)*, Hong Kong, China, Apr. 2003, vol. 6, pp. 109–112.

[5] B. Vo and S. Nordholm, "Non-Uniform DFT Filter Bank Design with Semi-Definite Programming," in *Proc. of Intl. Symposium on Signal Processing and Information Technology (ISSPIT)*, Darmstadt, Germany, Dec. 2003, pp. 42–45.

[6] M. Kappelan, *Eigenschaften von Allpaß-Ketten und ihre Anwendung bei der nicht-äquidistanten spektralen Analyse und Synthese*, Ph.D. thesis, RWTH Aachen University, Aachen, 1998, (in German).

[7] B. Shankar M. R. and A. Makur, "Allpass Delay Chain-Based IIR PR Filterbank and Its Application to Multiple Description Subband Coding," *IEEE Trans. on Signal Processing*, vol. 50, no. 4, pp. 814–823, Apr. 2002.

[8] C. Feldbauer and G. Kubin, "Critically Sampled Frequency-Warped Perfect Reconstruction Filterbank," in *Proc. of European Conference on Circuit Theory and Design (ECCTD)*, Cracow, Poland, Sept. 2003, vol. 3, pp. 109–112.

[9] E. Galijašević and J. Kliewer, "Design of Allpass-Based Non-Uniform Oversampled DFT Filter Banks," in *Proc. of Intl. Conference on Acoustics, Speech, and Signal Processing (ICASSP)*, Orlando (Florida), USA, May 2002, vol. 2, pp. 1181–1184.

[10] M. Parfieniuk and A. Petrovsky, "Reduced Complexity Synthesis Part of Non-Uniform Near-Perfect-Recontruction DFT Filter Bank Based on All-Pass Transformation," in *Proc. of European Conference on Circuit Theory and Design (ECCTD)*, Cracow, Poland, Sept. 2003, vol. 3, pp. 5–8.

[11] M. Parfieniuk, A. Petrovsky, and W. Wan, "Frequency Warping and Subband Merging for Approximating the Critical Bands with Cosine-Modulated Filter Banks," in *Proc. of Intl. Conference on Audio, Language and Image Processing (ICALIP)*, Shanghai, China, July 2008, pp. 1159 – 1166.

[12] H. W. Löllmann and P. Vary, "Parametric Phase Equalizers for Warped Filter-Banks," in *Proc. of European Signal Processing Conference (EUSIPCO)*, Florence, Italy, Sept. 2006.

[13] H. W. Löllmann and P. Vary, "Improved Design of Oversampled Allpass Transformed DFT Filter-Banks with Near-Perfect Reconstruction," in *Proc. of European Signal Processing Conference (EUSIPCO)*, Poznan, Poland, Sept. 2007, pp. 50–54.

[14] H. W. Löllmann, G. Dartmann, and P. Vary, "General Least-Squares Design of Allpass Transformed DFT Filter-Banks," in *Proc. of European Signal Processing Conference (EUSIPCO)*, Glasgow, UK, Aug. 2009, pp. 2653–2657.

[15] H. W. Löllmann and P. Vary, "Least-Squares Design of DFT Filter-Banks based on Allpass Transformation of Higher Order," *IEEE Trans. on Signal Processing*, vol. 58, no. 4, pp. 2393–2398, Apr. 2010.

[16] R. E. Crochiere and L. R. Rabiner, *Multirate Digital Signal Processing*, Prentice-Hall, Englewood Cliffs, New Jersey, 1983.